IOPscience iopscience.iop.org

Home Search Collections Journals About Contact us My IOPscience

# Monodispersed MnO nanoparticles with epitaxial $Mn_3O_4$ shells

This content has been downloaded from IOPscience. Please scroll down to see the full text.

2008 J. Phys. D: Appl. Phys. 41 134007

(http://iopscience.iop.org/0022-3727/41/13/134007)

View the table of contents for this issue, or go to the journal homepage for more

Download details:

IP Address: 128.32.220.242
This content was downloaded on 15/11/2013 at 02:45

Please note that terms and conditions apply.

J. Phys. D: Appl. Phys. **41** (2008) 134007 (5pp) doi:10.1088/0022-3727/41/13/134007

# Monodispersed MnO nanoparticles with epitaxial $Mn_3O_4$ shells

**A E Berkowitz[1,2], G F Rodriguez[1], J I Hong[2], K An[3], T Hyeon[3], N Agarwal[4], D J Smith[4] and E E Fullerton[2,5]**

[1] Department of Physics, University of California, San Diego La Jolla, CA 92093, USA
[2] Center for Magnetic Recording Research, University of California-San Diego La Jolla, CA 92093, USA
[3] National Creative Research Initiative Center for Oxide Nanocrystalline Materials, Seoul National University, Seoul 151-744, Korea
[4] School of Materials and Department of Physics, Arizona State University, Tempe, AZ 85287, USA
[5] Department of Electrical and Computer Engineering, University of California, San Diego La Jolla, CA 92093, USA

Received 14 January 2008, in final form 16 January 2008
Published 19 June 2008
Online at stacks.iop.org/JPhysD/41/134007

**Abstract**
We report the microstructural and magnetic properties of monodispersed nanoparticles (NPs) of antiferromagnetic MnO ($T_N = 118$ K), with epitaxial ferrimagnetic $Mn_3O_4$ ($T_C = 43$ K) shells. Above $T_C$, an unusually large magnetization is present, produced by the uncompensated spins (UCSs) on the surface of the MnO particles. These spins impart a net anisotropy to the MnO particles that is approximately three orders of magnitude larger than the bulk value. As a result, an anomalously high blocking temperature is exhibited by the MnO particles, and finite coercivity and exchange bias are present above $T_C$. When field cooled below $T_C$, a strong exchange bias was established in the $Mn_3O_4$ shells as a result of high net anisotropy of the MnO particles. A large coercivity was also observed. Models of several aspects of the behaviour of this unusual system emphasized the essential role of the UCSs on the surfaces of the MnO NPs.

(Some figures in this article are in colour only in the electronic version)

## 1. Introduction

One of the most interesting features of antiferromagnetic (AFM) nanoparticles (NPs) is that their magnetization in large applied fields is much higher than that expected from the susceptibility of the corresponding bulk AFM materials [1]. There is a general acceptance of Néel's explanation that this is due to unequal numbers of occupied sites in the antiparallel AFM sublattices of the NPs, i.e. uncompensated spins (UCSs) [2]. It is not generally recognized that when Meiklejohn and Bean reported their discovery of exchange anisotropy in NPs of Co with an AFM CoO coating, they suggested that CoO interfacial UCSs were involved in the most novel manifestation of the interaction, namely, the exchange-bias field ($H_{EB}$), the shift of the hysteresis loop along the field axis when the NPs were field cooled below the CoO AFM ordering temperature [3]. More recently, it was shown that $H_{EB}$ in polycrystalline bilayers of CoO and permalloy could be quantitatively predicted from the calculated density of UCSs derived from the size and orientation of the interfacial CoO crystallites [4]. The significance of the UCSs in AFM NPs and crystallites is associated with the 2007 award of the Nobel Prize in Physics to Albert Fert and Peter Grünfeld for the discovery of giant magnetoresistance (GMR) [5]. The prominence of GMR is due to the enormous technological importance of GMR sensors in every modern computer, which is enabled by the $H_{EB}$ provided by AFM films [6].

The most comprehensive investigations of AFM NPs have been on oxides, principally $\alpha$-$Fe_2O_3$, NiO, CoO and MnO [1]. With rare exceptions, these AFM NPs have not been particularly monodispersed, nor have they had regular, well-defined morphology. The papers on MnO NP [7–13] have generally reported significant magnetization well below the bulk value of $T_N = 118$ K [14]. The properties of arc-evaporated Mn NPs oxidized in air were associated with the presence of MnO and $Mn_3O_4$ [15]. A very recent paper discussed the properties of a series of spheroidal particles ranging from the smallest $Mn_3O_4$ NPs to larger particles with MnO cores and $Mn_3O_4$ shells [16].

 © 2008 IOP Publishing Ltd Printed in the UK

This paper discusses the behaviour of monodispersed rhomboidal MnO NPs with epitaxial $Mn_3O_4$ shells. Microstructural and magnetic properties of these NPs were presented in a previous paper [17]. In this paper, the pivotal role of the UCSs on the surface of the MnO NPs in establishing the unusual properties of this system is examined in detail. The unique atomic microstructure and magnetic features of these NPs facilitate modelling their properties. $T_C$ of the ferrimagnetic $Mn_3O_4$ shell is 43 K [18], which is much lower than $T_N$ (= 118 K) of the AFM MnO core. This permits determining the properties of the MnO UCSs with measurements above $T_C$ ($Mn_3O_4$). Since the MnO–$Mn_3O_4$ interface is epitaxial, the location and nature of the cations providing the UCSs can be specified. From the spontaneous magnetization exhibited by the UCSs above $T_C$ ($Mn_3O_4$), a value for the average number of Bohr magnetons on each uncompensated spin can be calculated and compared with the moments of the surface cations. Since the emphasis is on the UCSs in the following sections, some features of the particles are only briefly described. More detailed discussions on these issues are found in [17] and references therein.

## 2. Sample preparation and microstructure

The NPs were prepared by thermal decomposition of an Mn-oleate complex in a high boiling-point organic solvent [19]. The $Mn_3O_4$ shells on the MnO cores may have been present in the initial preparation, or they may have developed from washing in various solvents, or during storage in hexane. Samples of washed particles were dried and mounted for SQUID measurements in Ag cups which were compressed to immobilize the particles.

The morphology and microstructure of the particles are shown in figure 1. The particles generally have rhomboidal shapes with average sizes of 26–28 nm, as seen in figure 1(*a*). Figure 1(*b*), at a higher resolution, shows that the NPs have an MnO core with an $Mn_3O_4$ shell that has an average thickness of ∼4 nm. The {1 1 1} lattice planes of the phases are clearly well aligned, and the (1 1 1) spacings are indicated. The NPs exhibited broad and shallow x-ray diffraction peaks at the [2 1 1], [1 0 3] and [2 2 0] $Mn_3O_4$ positions and broad electron diffraction rings with diameters consistent with the large $Mn_3O_4$ unit cell.

$Mn_3O_4$ is a native oxide of MnO, as reported for bulk [20] and np [21]. Thus an epitaxial relationship is not surprising. As discussed in detail in [17], the MnO/$Mn_3O_4$ epitaxy can be modelled as depicted in figure 2. Cation vacancies are the most common defect in MnO; this requires the presence of $Mn^{3+}$ for charge balance. This combination of vacancies and $Mn^{3+}$ cations creates the normal spinel structure and occupancy of $Mn_3O_4$. Consequently, both $Mn^{2+}$ and $Mn^{3+}$ cations occupy epitaxial interfacial sites, and some of these sites are vacant.

## 3. Magnetic properties

Figure 3 shows the temperature dependence of the spontaneous magnetization $\sigma_0$, the coercivity, $H_C$, and the exchange-bias

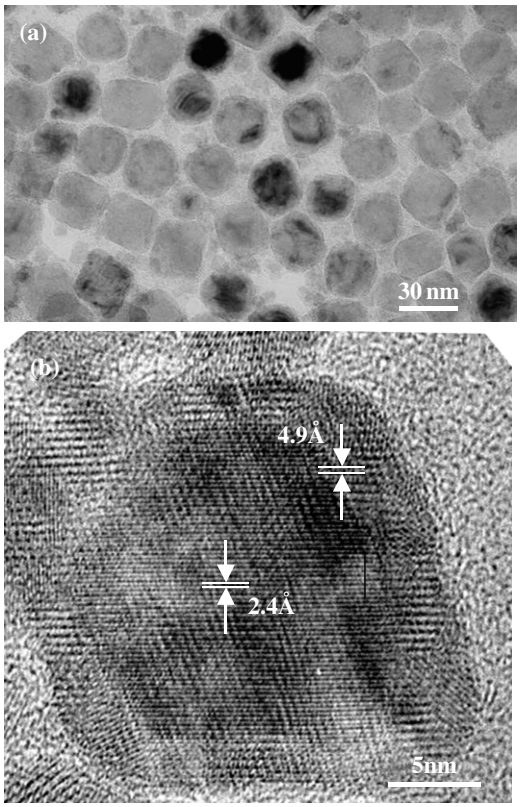


**Figure 1.** (*a*) Low magnification electron micrograph showing MnO/$Mn_3O_4$ NPs dispersed on thin carbon support film and (*b*) high resolution electron micrograph showing MnO/$Mn_3O_4$ NPs with excellent alignment of the {1 1 1} lattice planes of each phase.

field, $H_{EB}$. $\sigma_0$ was measured by extrapolating the high field magnetization back to $H = 0$. $H_C$ and $H_{EB}$ were measured from hysteresis loops recorded after field cooling (FC) in 50 kOe to 5 K. $H_C$ and $H_{EB}$ decrease rapidly with increasing temperature from large values at 5 K. $\sigma_0$ has a less precipitous temperature dependence. Remarkably, all three magnetic properties exhibit finite values above $T_C$ ($Mn_3O_4$) and do not vanish until much higher temperatures. In particular, $\sigma_0$ has a value at 43 K that is 20% of the value at 5 K.

Thermoremanent magnetization (TRM) was measured by cooling the NPs in 50 kOe to 10 K, reducing the field to zero and recording the remanence as the sample warmed (figure 4). TRM below 43 K was dominated by the remanence of the $Mn_3O_4$; above $T_C$($Mn_3O_4$), the UCS provided the TRM, and thereby monitored the superparamagnetic relaxation of the MnO NPs. The blocking temperature, $T_B$, of the MnO NPs was determined to be 95 K, as shown in the inset, from the nominal vanishing of the TRM.

For most magnetic NP systems, the susceptibility is measured in low fields, ⩽100 Oe, after FC in these fields or cooling in the zero field (ZFC), and the blocking temperature, $T_B$, is associated with the peak temperature of the ZFC data. With the present MnO/$Mn_3O_4$, this measurement was overwhelmed by the $Mn_3O_4$ signal. Therefore, the temperature dependence of the magnetization was measured in 50 kOe after cooling in 50 kOe, and after ZFC, with the results shown in figure 5. Measuring in such a high field ensures that the FC magnetization is saturated and that the ZFC values are

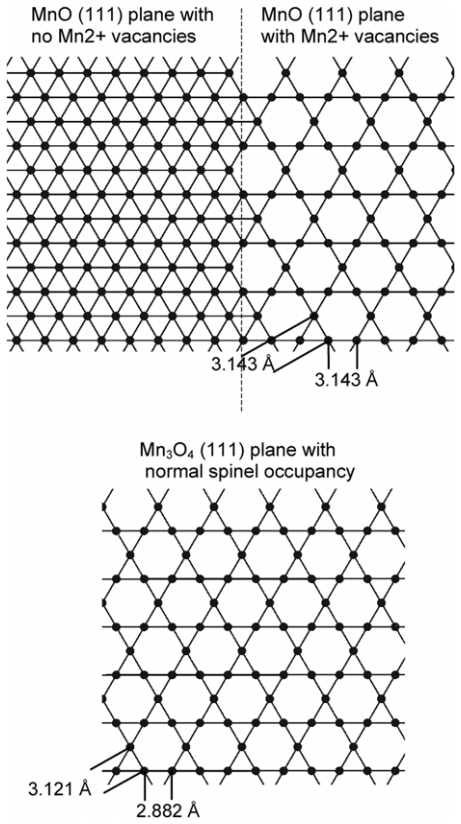


**Figure 2.** Site occupancy on (1 1 1) planes of MnO and $Mn_3O_4$. $Mn_3O_4$ cations are $Mn^{3+}$ in octahedral 'B' sites with normal spinel occupancy. With no vacancies, MnO sites are occupied by $Mn^{2+}$ cations. Cation vacancies produce $Mn^{3+}$ on Mn (1 1 1).

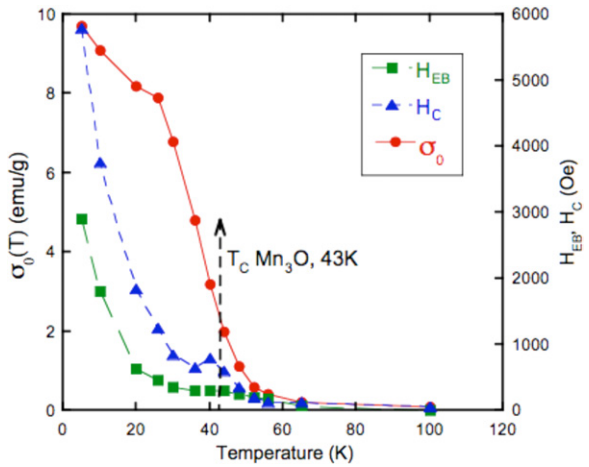


**Figure 3.** Temperature dependence of the spontaneous magnetization, $\sigma_0$, the coercivity, $H_C$, and the exchange-bias, $H_{EB}$, after cooling in 50 kOe.

completely reversible. Therefore the difference (FC − ZFC) is a valid measure of irreversibility below $T_B$. In the inset of figure 5, (FC − ZFC) is seen to vanish at 95 K, in agreement with the TRM determination of $T_B$.

## 4. Discussion

Above 43 K $T_C$ of ($Mn_3O_4$), the magnetic behaviour exhibited in figures 3–5 is attributed to the UCSs on the MnO NPs.

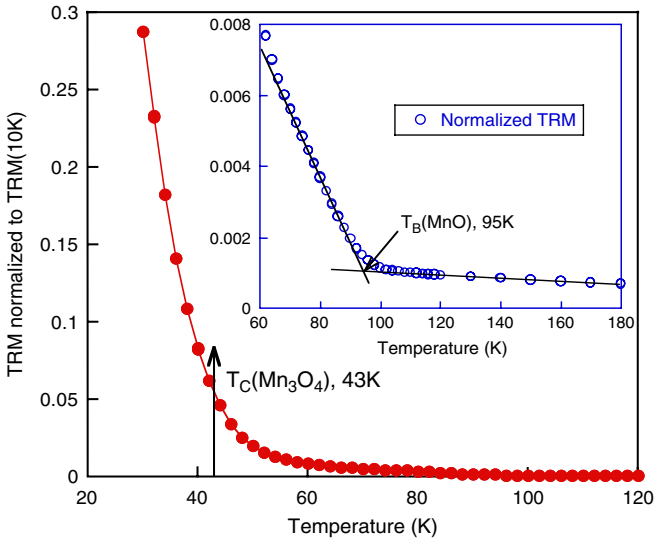


**Figure 4.** TMR after cooling in 50 kOe. Inset shows measurement of the temperature at which TMR vanishes.

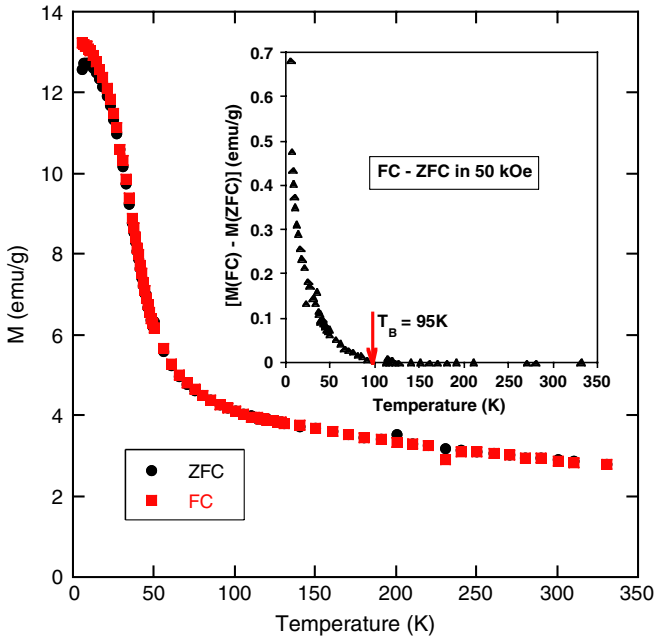


**Figure 5.** Temperature dependence of magnetization in 50 kOe after cooling in 50 kOe (FC) and after cooling in the zero field (ZFC). The enlarged view in the inset shows the temperature at which magnetization vanishes.

An alternative view is that the magnetization in this region is induced in the nominally paramagnetic $Mn_3O_4$ by the ordered MnO. This latter view does not clearly differ from a UCS model, since the surfaces of the MnO cores, where the UCS magnetization originates, can be specified to consist of epitaxial monolayers of $Mn^{2+}$ and $Mn^{3+}$ cations with some vacant sites. It is shown below that treating the magnetization at temperatures above 43 K as that of MnO UCSs, provides a consistent model for the unusual properties in this temperature region, as well as at lower temperatures.

The spontaneous magnetization at 43 K (figure 3) is taken to be the 'ground state' magnetization of the UCSs. In order to

compute the average moment of each uncompensated spin, an average particle is assumed to be a cube with 27 nm edges, an MnO cube core and a 4 nm $Mn_3O_4$ shell. Using the densities of the two phases and the MnO lattice spacing, a straightforward calculation yields the number of cation sites on the surfaces of the MnO cubes, per gram of sample. Dividing $\sigma_0$ by this number gives the result that, to two significant figures, the average number of Bohr magnetons on each uncompensated spin is $2.0\mu_B$. Aside from the amusing coincidence that the result of a computation involving $\sim 10^{14}$ particles resulted in a single digit number of Bohr magnetons, $2.0\mu_B$/UCS can be compared with the moments expected from the cations occupying the epitaxial interfaces, i.e. principally $Mn^{2+}$ and some $Mn^{3+}$. $Mn^{2+}$ has $5\mu_B$ and $1\mu_B$ in the high and low spin states, respectively; $Mn^{3+}$ has $1\mu_B$ less in each state. While it is likely that deviations from cubic crystal fields at the surfaces of the MnO cores would promote low spin states, no reliable estimate of the accuracy of the calculated average UCS moment can be inferred from the present data. However, it is clear that the calculated $2.0\mu_B$/UCS is comfortably within the range of possible values. The $2.0\mu_B$/UCS estimate is made on the basis that all interfacial cation sites are occupied. Even allowing for the fact that some sites are vacant (figure 2), this would be an unusually high occupancy for UCSs on AFM NPs. Generally, only a few per cent of the potential UCS sites are estimated to be occupied, e.g. CoO polycrystalline films [4]. The reason for the high occupancy in this case is that the FM/AFM interface is epitaxial, and the UCSs constitute a surface monolayer of the NPs. In turn, this latter fact supports the model of complete epitaxy, even though only {1 1 1} plane alignment is visible in figure 1(*a*).

The blocking temperature, $T_B$, was determined to be 95 K from both the vanishing of TRM (inset, figure 4), and the disappearance of irreversibility in 50 kOe FC and ZFC magnetization measurements (inset, figure 5). When this value is compared with that obtained from superparamagnetic relaxation considerations, it becomes clear that the MnO NPs have anomalously high anisotropies as compared with bulk values. For $T \rightarrow 0$ K, the anisotropy in the easy (1 1 1) plane of an MnO single crystal is $K_2 = 276\,\mathrm{erg\,cm^{-3}}$ [22]. It is generally accepted that for SQUID measurements that require about 1 min per point, the expression $KV/kT$, where $K$ is the anisotropy constant of NPs with volume $V$, should be about 25 for magnetic thermal stability. For the MnO NPs, $K_2V/kT = 3.4$ at 4 K, i.e. a vanishing blocking temperature. For stability at 95 K, the MnO NPs would require $K = 4.9\times10^4\,\mathrm{erg\,cm^{-3}}$ at 95 K, which implies that $K > 10^5\,\mathrm{erg\,cm^{-3}}$ at 4 K, three orders of magnitude higher than the bulk value. The low coordination of surface cations, surface cation vacancies and the presence of other surface defects have been shown to produce anomalously high values of anisotropy and disorder in various magnetic oxide NPs [23, 24]. Morales *et al* [11] have comprehensively examined the issue of surface-induced high anisotropy in MnO NPs and arrived at expressions for the ground state net anisotropy, $K_{eff}$, of MnO particles with $N$ total Mn atoms and $N_S$ surface Mn atoms. With no anisotropy correlations among the surface atoms, i.e. complete disorder, $K_{eff} = N_S^{1/2}K_0/N$; for no disorder, $K_{eff} = N_SK_0/N$. Here $K_0$ is the specific anisotropy energy per atomic volume contributing to the energy barrier. For the MnO NPs, $K_0$ is taken to be $2\times10^7\,\mathrm{erg\,cm^{-3}}$. For the present MnO NPs, these expressions yield: for complete disorder, $K_{eff} = 2.7\times10^4\,\mathrm{erg\,cm^{-3}}$; for no disorder, $K_{eff} = 2.8\times10^6\,\mathrm{erg\,cm^3}$. Since the measured $T_B$ implies a value of $K > 10^5$, a significant amount of surface disorder is suggested by these calculated boundary values.

A plausible model for $H_C$ above 43 K after FC is that the UCSs are polarized by the applied fields and, assisted by thermal excitation, exert sufficient torque on their respective single domain MnO NPs to switch the Néel axis irreversibly as the field is cycled. Thermal excitation reduces $H_C$, which remains finite until $T_B$ is reached. The origin of the apparent finite $H_{EB}$ above 43 K is more difficult to visualize. It does not seem reasonable to attribute the $H_{EB}$ above 43 K to the switching of exchange-biased UCSs, since it is these same UCSs that induce a large enough anisotropy in the MnO NPs to permit a finite $H_{EB}$. The apparent $H_{EB}$ could result from a vertical shift of $\sim\leqslant 1\%$ of the saturated magnetization of the hysteresis loops in that temperature region. Our measurements could not resolve a shift of that magnitude. However, the very large anisotropies of some UCSs, present as discussed above, could readily produce a strong enough moment, polarized by FC, to provide an upward shift of the hysteresis loops on the order of 1%.

Below 43 K, the $Mn_3O_4$ magnetization dominates. The $Mn_3O_4$ particles are essentially hollow rhomboids with a shell thickness of $\sim$40 Å. The $H_C$ values are quite large, although smaller than those of equi-axed $Mn_3O_4$ NPs with an average size of 15 nm [25], and they decrease more steeply with temperature. The large surface/volume ratios of these particles emphasize the role of surface anisotropy. Spin disorder on the outer surfaces is likely present and contributes to the net anisotropy. The large anisotropies on the inner surfaces were discussed above. Certainly the very high $c$-axis anisotropy of $Mn_3O_4$ is an important energy barrier, since it is likely to be involved in any magnetization reversal in these hollow rhomboids. The magnetic switching processes of hollow rhomboidal $Mn_3O_4$ particles are clearly a separate complex issue that needs attention, possibly along the lines of the recent work on hollow spheres [26].

$H_{EB}$ is also large at 5 K and decreases rapidly with temperature. Its significant magnitude is a strong support of the model that the MnO NPs can be regarded as having a net effective anisotropy much larger than the bulk due to the contributions of the surface cations, thereby supporting a large $H_{EB}$ in the $Mn_3O_4$ shell. The MnO UCSs are also responsible for establishing $H_{EB}$, as well as supporting it. Field-cooled from above $T_N$, the polarized UCSs polarize the $Mn_3O_4$, induce a high net anisotropy in the MnO NPs, and provide the interfacial $Mn_3O_4$-MnO exchange link.

## 5. Summary

Due to their unique magnetic and atomic microstructures, these AFM MnO NPs with their native-oxide, epitaxial, ferrimagnetic $Mn_3O_4$ shells present a number of magnetic properties that are quite unusual for AFM NPs. Since

$T_N$(MnO) is much greater than $T_C(Mn_3O_4)$, measurements above $T_C(Mn_3O_4)$ permit the investigation of the properties of a sample of relatively monodispersed AFM NPs. Since the MnO–$Mn_3O_4$ interface is epitaxial, the interfacial cation occupancy can be specified with some confidence. A large moment per interfacial cation site is found, which implies an unusually high UCS surface-site occupancy. These features are due to the epitaxial nature of the MnO–$Mn_3O_4$ interface. The UCSs on the MnO NP surfaces induce an effective anisotropy in the MnO NPs that is approximately three orders of magnitude greater than the bulk MnO value. This effective MnO anisotropy is responsible for the large exchange bias below $T_C(Mn_3O_4)$, and contributes to the coercivity. Above $T_C(Mn_3O_4)$, the effective MnO anisotropy produces a blocking temperature near $T_N$(MnO), whereas the bulk anisotropy would not yield a finite blocking temperature. $H_C$ above $T_C(Mn_3O_4)$ results from the irreversible switching of the spin lattices of the MnO NPs by the torque exerted by the UCSs as the applied field is cycled. $H_{EB}$ at high temperatures could be due to a 1% upward shift of the hysteresis loops by polarized, high anisotropy UCSs after FC. Thus, virtually all of the anomalous behaviour in this NP system can be ascribed to the properties of the interfacial UCSs.

## Acknowledgments

The authors acknowledge the use of facilities in the John M. Cowley Center for High Resolution Electron Microscopy at Arizona State University. The partial support and the use of the facilities of the Center for Magnetic Recording Research are gratefully appreciated.

## References

[1] Mørup S, Madsen D E, Frandsen C, Bahl C R H and Hansen M F 2007 *J. Phys.: Condens. Matter* **19** 213202
[2] Néel L 1961 *C.R. Acad. Sci. Paris* **252** 4075
[3] Meiklejohn W H and Bean C P 1957 *Phys. Rev.* **105** 90
[4] Takano K, Kodama R H, Berkowitz A E, Cao W and Thomas G 1997 *Phys. Rev. Lett.* **79** 1130
[5] http://nobel_prizes/physics/laureates/2007/index.html
[6] Dieny B, Speriosu V S, Parkin S S P, Gurney B A, Wilhoit D R and Mauri D 1991 *Phys. Rev.* B **43** 1297
[7] Seo W S, Jo H H, Lee K, Kim B, Oh S J and Park J T 2004 *Angew. Chem.* **116** 1135
[8] Lee G H, Huh S H, Jeong J W, Choi B J, Kim S H and Ri H -C 2002 *J. Am. Chem. Soc.* **124** 12094
[9] Chang Y Q, Yu D P, Wang Z, Long Y, Zhang H Z and Ye R C 2005 *J. Cryst. Growth* **281** 678
[10] Masala O and Seshadri R 2005 *J. Am. Chem. Soc.* **127** 9354
[11] Morales M A, Skomski R, Fritz S, Shelburne G, Shield J E, Yin M, O'Brien S and Leslie-Pelecky D L 2007 *Phys. Rev.* B **75** 134423
[12] Yin M and O'Brien S 2003 *J. Am. Chem. Soc.* **125** 10180
[13] Sak S and Ohshima K 1995 *J. Phys. Soc. Japan* **64** 955
[14] Kantor A P, Dubrovinsky L S, Dubrovinskaia N A, Kantor L Y and Goncharenko L N 2005 *J. Alloys. Compounds* **402** 42
[15] Si P Z, Li D, Lee J W, Choi C J, Zhang Z D, Geng D Y and Brück E 2005 *Appl. Phys. Lett.* **87** 133122
[16] Salazar-Alvarez G, Sort J, Surinach S, Dolors Baro M and Nogés J 2007 *J. Am. Chem. Soc.* **129** 9102
[17] Berkowitz A E, Rodriguez G F, Hong J I, An K, Hyeon T, Agarwal N, Smith D J and Fullerton E E 2008 *Phys. Rev.* B **77** 024403
[18] Robie R A and Hemmingway B S 1985 *J. Chem. Thermodyn.* **17** 165
[19] Park J, An K, Hwang Y, Park J-G, Noh H-J, Kim J-Y Park J-H, Hwang N-M and Hyeon T 2004 *Nature Mater.* **3** 891
[20] Jagadeesh M S and Seehra M S 1980 *Phys. Rev.* B **21** 2897
[21] Park J, Kang E, Bae C J, Park J-G, Noh H-J, Kim J-Y, Park J-H, Park H M and Hyeon T 2004 *J. Phys. Chem.* B **108** 13594
[22] Jagadeesh M S and Seehra M S 1981 *Phys. Rev.* B **23** 1185
[23] Kodama R H 1999 *J. Magn. Magn. Mater.* **200** 359
[24] Fiorani D (ed) 2005 *Surface Effects in Magnetic Nanoparticles* (Berlin: Springer)
[25] Winkler E, Zysler R D and Fiorani D 2004 *Phys. Rev.* B **70** 174406
[26] Goll D, Berkowitz A E and Bertram H N 2004 *Phys. Rev.* B **70** 184432